

# Photocatalytic Oxidation of Aromatic Pollutants and Electrochemical Behavior in Water Over Nanopolyphosphotungstate Supported on $\text{In}_2\text{O}_3$

Hossein Salavati\*, Hamide Saedi

Department of Chemistry, Payame Noor University (PNU), 19395-3697, Tehran, I.R.Iran

\*E-mail: [hosseinsalavati@pnu.ac.ir](mailto:hosseinsalavati@pnu.ac.ir)

Received: 18 September 2014 / Accepted: 16 October 2014 / Published: 23 March 2015

---

So far, useful advanced oxidation procedures have been used for mineralizing natural contaminants in aqueous media via irradiating of the nanocomposites by ultraviolet irradiation and ultrasound waves; photocatalysis and sonocatalysis are just a few cases. Polyphosphotungstate /Indium oxide was made ready by the use of sol-gel strategy and recognized by using X-Ray Diffraction, Fourier-Transformed Infra-Red spectroscopy, Ultraviolet-Visible spectroscopy, Scanning Electron Microscopy and elemental analysis. In the present study, the photocatalytic and sonocatalytic actions of the reinforced polyphosphotungstate were examined by the use of degradation of different dyes (Methylene Blue, Bromothymol Blue, Methyl Orange, Solophenyl Red-3BL, and Nylosan Black 2-BC). The polyphosphotungstate /Indium oxide nanocomposite revealed more photocatalytic and sonocatalytic action than pure polyphosphotungstate or pure Indium oxide.

---

**Keywords:** Photocatalysis, Aromatic pollutants, Sol-gel, Nanocomposites, Oxidation

## 1. INTRODUCTION

Heterogeneous photocatalytic devastation of natural contaminants in wastewater by using UV light as the excitation energy is an eye-catching area which draws an excellent attention recently [1–5]. In this respect, production of the efficient photocatalytic substances which has been both a challenge and opportunity for chemists is of vital importance. Indium oxide ( $\text{In}_2\text{O}_3$ ) is one of the most commonly investigated heterogeneous semiconductor photocatalysts, since heteropolyacids (HPAs) have been analyzed as homogeneous photocatalysts [6–10]. Both  $\text{In}_2\text{O}_3$  and HPAs have very identical photocatalytic processes in common due to their identical electronic features. Although HPAs show UV-light photocatalytic measures in the homogenous methods, the main drawbacks of them as

photocatalysts are their low surface area and complexity in isolating them from the response mixture. Therefore, enlargement of novel solid catalysts with important features such as surface area and porosity, have been a dispute for a long period. As for the applicability of this strategy, also, immobilization of dissolvable HPA into some matrixes for preparing solid or reinforced HPA photocatalysts is important. In comparison with the pure or homogeneous HPAs, these insoluble HPA/ $\text{In}_2\text{O}_3$  nanocomposites show much more UV-photocatalytic action. Moreover, separation of these components and restoring them for recycling objective can be carried out with much more convenience. To be able to enhance the photoefficiency of either HPAs or  $\text{In}_2\text{O}_3$ , and immobilization of dissolvable HPAs, nanocomposites of polyphosphotungstate /Indium oxide ( $\text{H}_3\text{PW}_{12}\text{O}_{40}/\text{In}_2\text{O}_3$ ) have been made ready via mixing the methods of sol-gel and hydrothermal behavior. That is, HPA has been vacant d orbits and can be used as good electron acceptors. After the addition of HPA to  $\text{In}_2\text{O}_3$  photocatalytic methods, the speed of the charge pair recombination can be decreased considerable. Thus, HPA can increase the rate of the conduction band (CB) electron exchange by accepting e- (photogenerated electrons) to its vacant d orbits. Latest research have indicated that colors can be removed from the reactive dyes by the advanced oxidation process [11]; In this process, solid oxidizing agents like hydroxyl radicals ( $\text{OH}^\circ$ ) are developed, which entirely eliminate the contaminants in wastewater. The hydroxyl radicals can mineralize almost all of the natural compounds into  $\text{CO}_2$  and  $\text{H}_2\text{O}$  and into other simple inorganic ions. One of the eye-catching advanced oxidation procedures is heterogeneous photocatalysis through the radiation of UV [12] or solar light [13] on a semiconductor surface. The ultrasound energy can have any or all of the following effects on chemical activity: production of heat, promotion of the mixing or mass transfer, increase of the close contact between components, dispersion of contaminated layers of the chemicals, and the production of free-chemical radicals. The physical effect of ultrasound examination can enhance the reactivity of a catalyst by widening the surface area or speeding up a response by a proper combination the reagents. The chemical effects of ultrasound examination increase response rates because of the development of extremely sensitive radical varieties formed during cavitation. Indeed, the observed desorption of natural varieties from the semiconductor surface might also have some part, even if not actually positive, in changing the deterioration rate under photocatalysis. In this methods sound or ultrasound waves are used to generate an oxidative atmosphere via cavitation and this, in turn, results in localized microbubbles and supercritical areas in the aqueous phase. The burst of these bubbles produces amazingly high local temperature and pressure. These rather extreme conditions cannot last for long but it has been indicated that some extremely sensitive varieties such as hydroxyl ( $\text{OH}^\circ$ ), hydrogen ( $\text{H}^\circ$ ) and hydroperoxyl ( $\text{HO}_2^\circ$ ) radicals, and remove the color can be developed under such conditions. These radicals can trigger or promote many quick reduction-oxidation responses. These responses with inorganic and natural substrates are quick and often approximate the diffusion-controlled rate [14, 15]. In this paper, we wish to report, the preparation of the polyphosphotungstate-Indium oxide ( $\text{H}_3\text{PW}_{12}\text{O}_{40}/\text{In}_2\text{O}_3$ ) nanocomposite by sol-gel process and its application as a heterogeneous photocatalyst and sonocatalyst for efficient degradation of different dyes into corresponding inorganic products.

## 2. MATERIALS AND METHODS

### 2.1. Materials and instruments

The chemicals used were all in analytical grade without any filtration. For Elemental analysis and Atomic absorption analysis, a Perkin-Elmer 2400 device and a Shimadzu 120 spectrophotometer were used respectively.

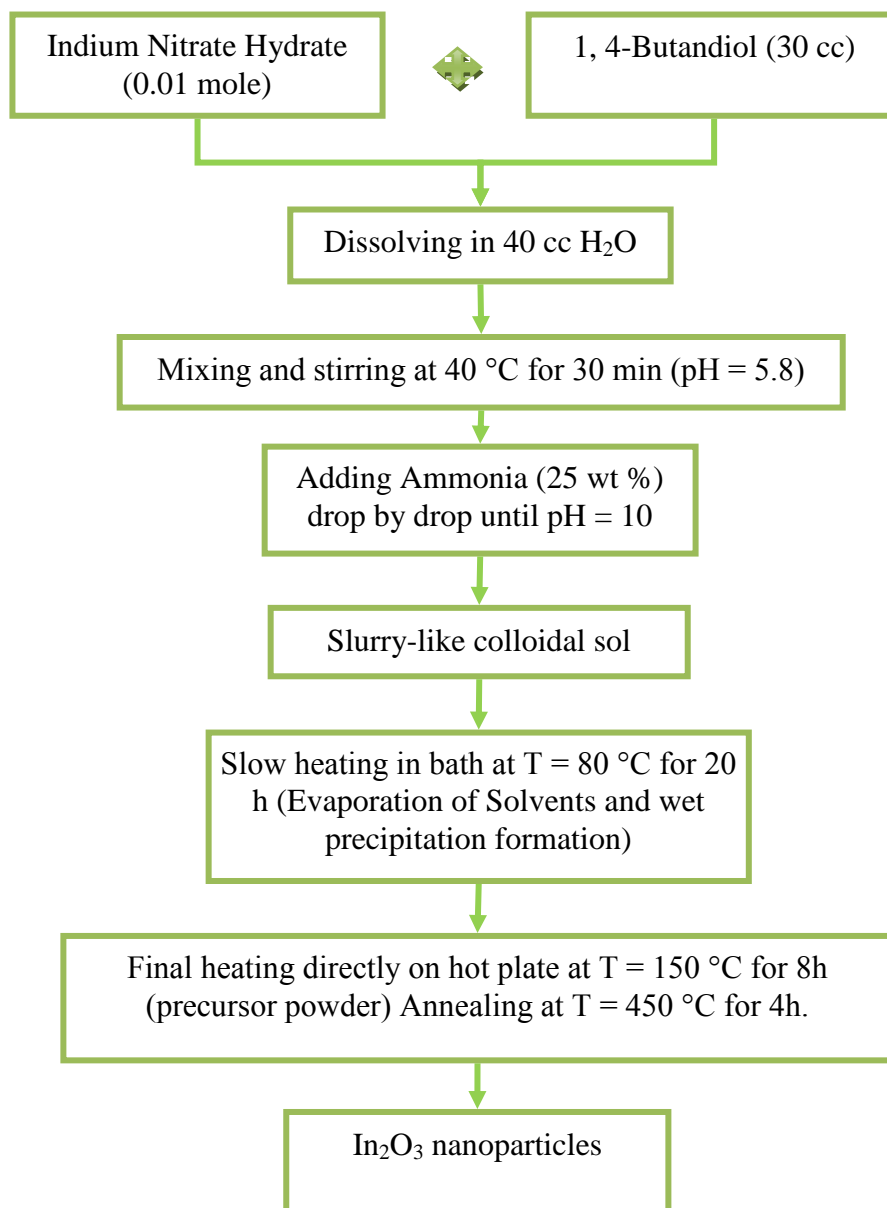


**Figure 1.** The flow chart for preparation of In<sub>2</sub>O<sub>3</sub> nanoparticles by the hydro-thermal process

Diffuse reflectance spectra (DRS) were read on a Shimadzu UV-265 device with visual quality BaSO<sub>4</sub> as the criterion. The light emitted from a 400 W high-pressure mercury lamp over the range from 200-400 nm. Fourier-transformed infrared (FTIR) spectra were acquired as potassium bromide

pellets over the range from 400-4000  $\text{cm}^{-1}$  with Nicolet-Impact 400D device. Scanning electron micrographs (SEM) of the catalyst and reinforcement were taken using SEM Philips XL 30. Powder X-ray diffraction (XRD) were measured on a D<sub>8</sub> Advanced Bruker, using Cu K $\alpha$  rays ( $2\theta=5-70^\circ$ ). Cyclic voltammetric (CV) analysis were conducted with an Auto Lab 30 device.

## 2.2. Synthesis of $\text{In}_2\text{O}_3$ nanoparticles hydrothermal method

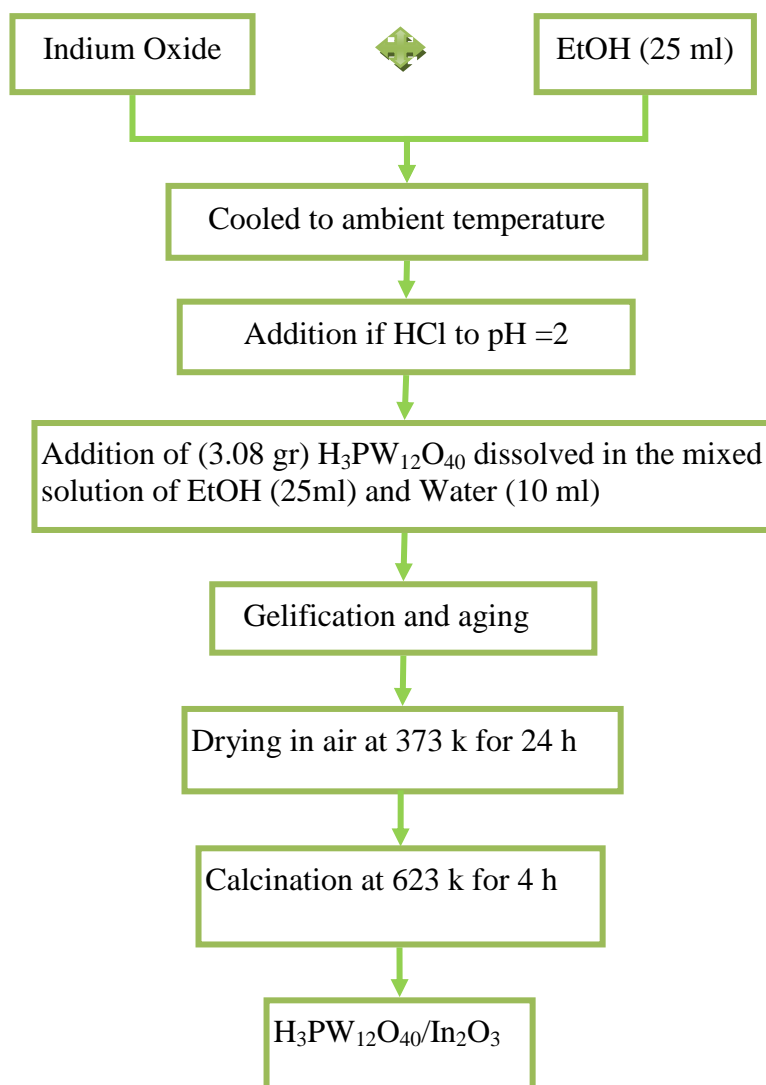
$\text{In}_2\text{O}_3$  nanoparticles were synthesized by a hydrothermal method, as summarized in Fig.1, in hydrothermal method, 0.01 mole indium nitrate hydrate was dissolved in 40 cc deionization water and 30 cc 1, 4-butanediol as dispersing agent [6]. Then, the solution with pH = 5.8 was stirred for 30 min at  $T = 40^\circ\text{C}$ . Ammonia (25 wt %) was instilled in the solution until a final pH = 10 was obtained at room temperature. After the formation of white slurry like colloidal sol, the mixture was heated continuously at the constant temperature of  $T = 80^\circ\text{C}$  for 10 h in an open bath until the solvent was evaporated and a light-brown wet solid was left. In this hydrothermal process,  $\text{In}^{3+}$  ions and ammonia (as mineralizer) have the chemical reactions, necessary for the preparation of  $\text{In}_2\text{O}_3$  powders [16]. In the final stage, the wet precipitation was fully dried by direct heating on the hot plate at  $T = 150^\circ\text{C}$  for 8 h. A white-grey powder is the final product of the reaction.

## 2.3. Post-annealing of the $\text{In}_2\text{O}_3$ nanoparticles

After the hydrothermal method, fine powders were obtained by grinding the precursor powders in the glassy mortar. Then, powders were heated in a pyrex crucible to  $T = 450^\circ\text{C}$  and calcined for 8 h, in an electric box furnace, and finally cooled down to reach the room temperature. In this way, post-annealing of the powders completely decomposed all the organic compounds, and  $\text{In}_2\text{O}_3$  nanoparticles were obtained (Fig. 1).

## 2.4. Synthesis of $\text{H}_3\text{PW}_{12}\text{O}_{40}/\text{In}_2\text{O}_3$ nanocomposite by sol-gel method

An  $\text{In}_2\text{O}_3$  . ethanol solution (25 mL) was stirred at  $80^\circ\text{C}$ , and then the mixture was slowly cooled back to ambient temperature. Afterward, hydrochloric acid was used to adjust the acidity of the mixture to pH=2. To the resulting mixture,  $\text{H}_3\text{PW}_{12}\text{O}_{40}$  (3.08 g) which was dissolved in the mixed solution of 25 mL ethanol and 10 mL of water was added dropwise, and was maintained under constant stirring for 3 h until the gelling point was reached. After the gelation phase, the solid was filtered and dried in air at  $100^\circ\text{C}$  for 24h. The dried gel went through a 4h vacuum calcination at  $350^\circ\text{C}$  for the  $\text{In}_2\text{O}_3$  network to be made and then, it was washed with hot water ( $80^\circ\text{C}$ ) three times (Fig. 2).

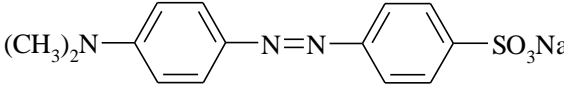
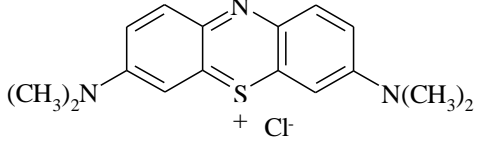
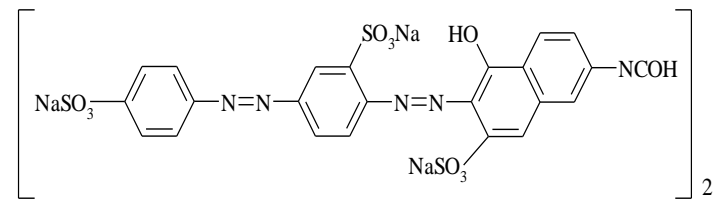
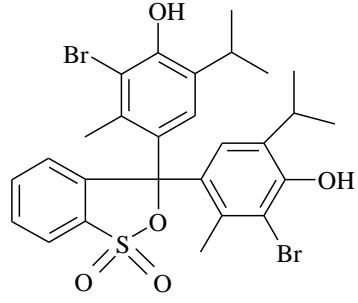
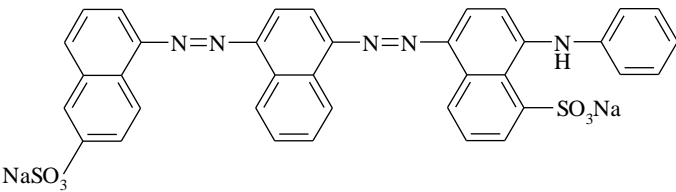


**Figure 2.** The flow chart for preparation of  $\text{H}_3\text{PW}_{12}\text{O}_{40}/\text{In}_2\text{O}_3$  nanocomposite by sol-gel method

### 2.5. General procedure for photocatalytic degradation of dyes

Several dyes including Nylosan Black 2-BC, Methyl Orange, Solophenyl Red-3BL, Bromothymol Blue and Methylene Blue were used as the target for testing the catalytic activity of the nanocomposite. A general photocatalytic method was carried out as follows: A suspension of 20 mg  $\text{H}_3\text{PW}_{12}\text{O}_{40}/\text{In}_2\text{O}_3$  nanocomposite in 10 mL fresh aqueous dye solution was made. After the stability of the suspension intensity the lamp was inserted around it. Photodegradation of dye was carried out in an open container using oxygen as the oxidant. After the end of the reaction the suspensions went under the process of centrifugation and filtration; the photolyte was analyzed by UV-vis spectrophotometer at  $\lambda_{\text{max}}$  for each dye. The structure of dyes and their  $\lambda_{\text{max}}$  are offered in Table 1.

**Table 1.** Dyes structure used in this study

Dye	Chemical formula	MW	$\lambda_{\max}$ (g/mol)
Methyl Orange (MO)		327.34	462
Methylene Blue (MB)		373.88	663
Solophenyl Red-3BL		1373.3	530
Bromothymol Blue		624.40	435
Nylosan Black 2-BC		731.26	570

## 2.6. General procedure for dyes degradation under ultrasonic irradiation

As for sonication, a UP 400S ultrasonic processor with the operating frequency of 24 kHz was immersed directly into the reaction mixture. The total volume of the solution was 10 mL. A suspension was prepared by 20 mg of  $\text{H}_3\text{PW}_{12}\text{O}_{40}/\text{In}_2\text{O}_3$  nanocomposite in 10 mL of fresh aqueous dye solution. Then, ultrasonic waves were used for sonicating the solution reaction. At the end of the reaction, the

suspensions went under centrifugation and filtration, and for each dye then the photolyte was analyzed by UV–vis spectrophotometer at  $\lambda_{\max}$ .

### 3. RESULTS AND DISCUSSION

#### 3.1. Catalyst description

It is recognized that the catalytic activity of nanocomposites is strongly dependent upon the shape, size and size distribution among the particles. Therefore, describing the microstructure of the nanocomposite is of vital importance. Fig. 3 shows the SEM images of the  $\text{In}_2\text{O}_3$  nanoparticles and  $\text{H}_3\text{PW}_{12}\text{O}_{40}/\text{In}_2\text{O}_3$  nanocomposite. SEM image reveals that powder is composed of aggregated extremely fine particles. As it is clear from the image, particles have a homogeneous shape. The particles' sizes of the  $\text{In}_2\text{O}_3$  and  $\text{H}_3\text{PW}_{12}\text{O}_{40}/\text{In}_2\text{O}_3$  nanocomposite prepared by a sol-gel method 36 and 38 nm respectively.

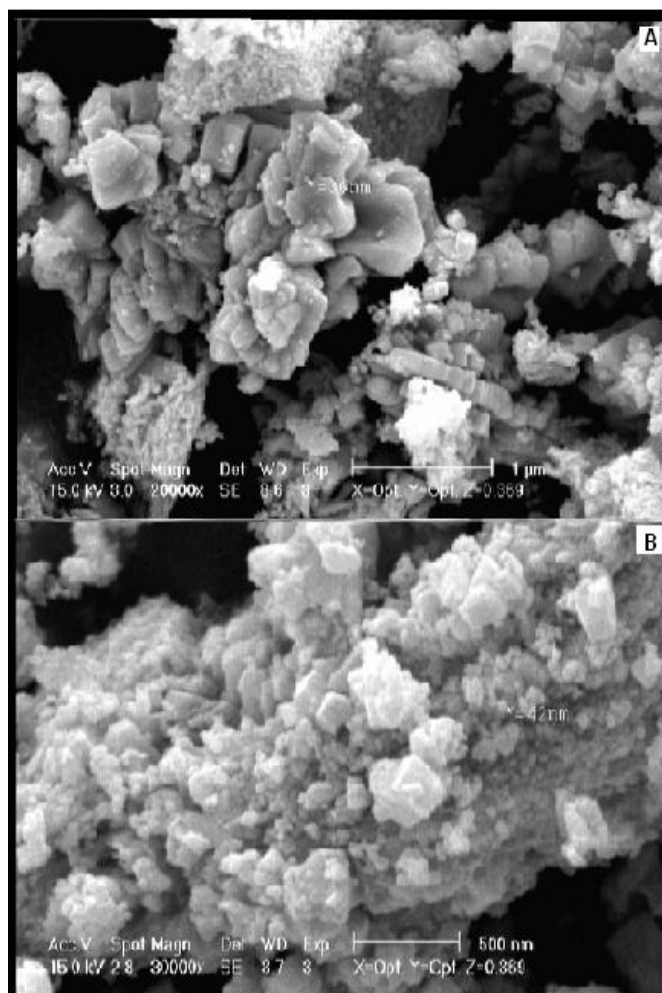


**Figure 3.** The SEM image of (a)  $\text{In}_2\text{O}_3$  nanoparticles prepared by the hydrothermal process ;( b)  $\text{H}_3\text{PW}_{12}\text{O}_{40}/\text{In}_2\text{O}_3$  prepared by sol-gel process.

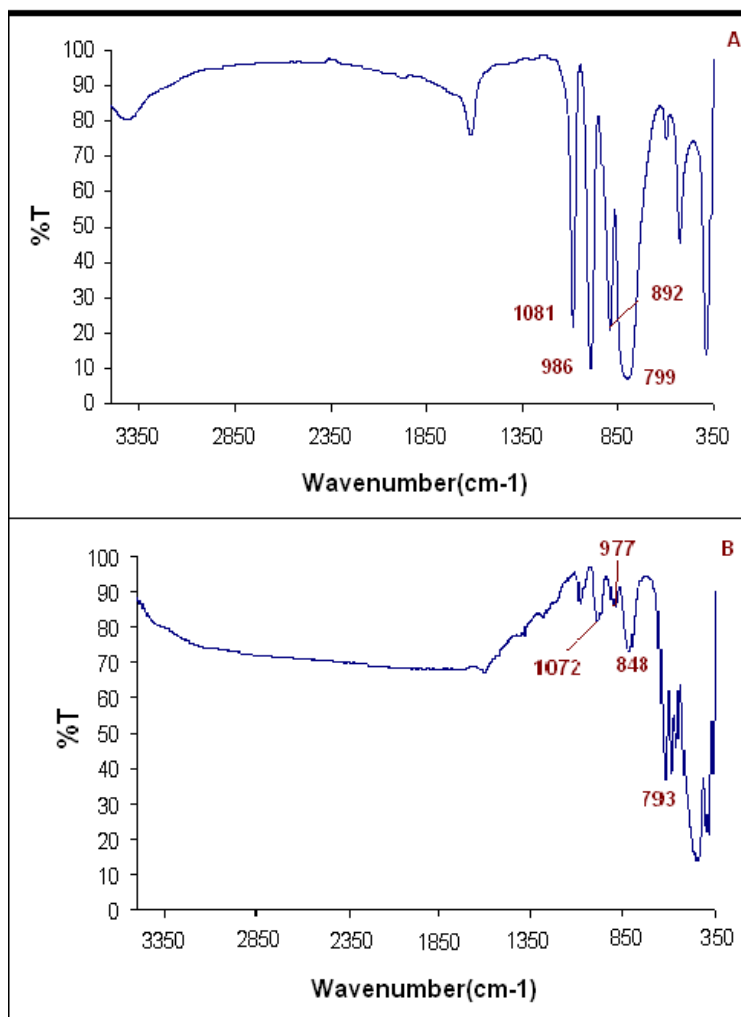


**Figure 4.** The FT-IR patterns of (a)  $\text{H}_3\text{PW}_{12}\text{O}_{40}$ ; (b)  $\text{H}_3\text{PW}_{12}\text{O}_{40}/\text{In}_2\text{O}_3$  nanocomposite

The FT-IR spectrum of  $\text{H}_3\text{PW}_{12}\text{O}_{40}$  had been shown in Fig.4a, at (799), (892), (986) and (1081)  $\text{cm}^{-1}$  corresponding to the W-O<sub>c</sub>-W, W-O<sub>e</sub>-W, W=O and P-O bonds respectively. Fig. 4b shows the FT-IR spectrum of the  $\text{H}_3\text{PW}_{12}\text{O}_{40}/\text{In}_2\text{O}_3$  nanocomposite, The FT-IR typical bands of HPA in the HPA/  $\text{In}_2\text{O}_3$  nanocomposite have some red shifts compared with those for the pure HPA [17, 18]. This confirms the existence of a strong chemical interface, not a simple physical incorporation between the polyoxometalate and  $\text{In}_2\text{O}_3$  surface.

The XRD patterns of  $\text{H}_3\text{PW}_{12}\text{O}_{40}$  and  $\text{H}_3\text{PW}_{12}\text{O}_{40}/\text{In}_2\text{O}_3$  have been shown in Fig.5, respectively. The characteristic diffraction peaks at the XRD patterns of  $\text{H}_3\text{PW}_{12}\text{O}_{40}$  at (10.5), (25.5), (29.5) and (35), are observed in the XRD patterns of  $\text{H}_3\text{PW}_{12}\text{O}_{40}/\text{In}_2\text{O}_3$  with lower intensity. There are, also, some alterations occurred in the peak positions and widths. It is clear that the changes are for immobilization of HPA into a matrix  $\text{In}_2\text{O}_3$ ; The mean of the particle size for  $\text{H}_3\text{PW}_{12}\text{O}_{40}/\text{In}_2\text{O}_3$  powder was estimated based on XRD line broadening by the application of the Debye–Scherer formula,  $D = (0.89\lambda) / (\beta/2\cos\theta)$ , where  $\lambda$  is the wavelength for Cu  $K_\alpha$  rays,  $\beta/2$  is the full width of half maximum (FWHM) and  $\theta$  is the Bragg angle. The range from the particle size calculated is about 17.00-19.00 nm.

For the purpose of examining the electrochemical behavior of the water insoluble HPA which has been reinforced on  $\text{In}_2\text{O}_3$ , a three dimensional bulk- modified carbon paste electrode (CPE) was made employing the supported catalyst. The electrode was prepared by mixing the graphite powder as the conductive material, silicon oil as the pasting liquid, and reinforced HPAs as the electroactive varieties. Because of the instability of HPA in neutral and basic aqueous solutions, the electrochemical experiments were conducted in 0.2 M  $\text{H}_2\text{SO}_4$  aqueous solution. Fig. 6 shows the cyclic voltammogram in 0.2 M  $\text{H}_2\text{SO}_4$  aqueous solution at a bare CPE, and CPE modified with HPA -  $\text{In}_2\text{O}_3$ . It can be observed that in the potential range of -0.50 to 0.1 V (vs. Ag/AgCl) there is no redox peak at the bare CPE, while some consecutive redox processes are observed at the modified CPE. The above experimental results showed that HPA can be reinforced on the surface of  $\text{In}_2\text{O}_3$  [19].

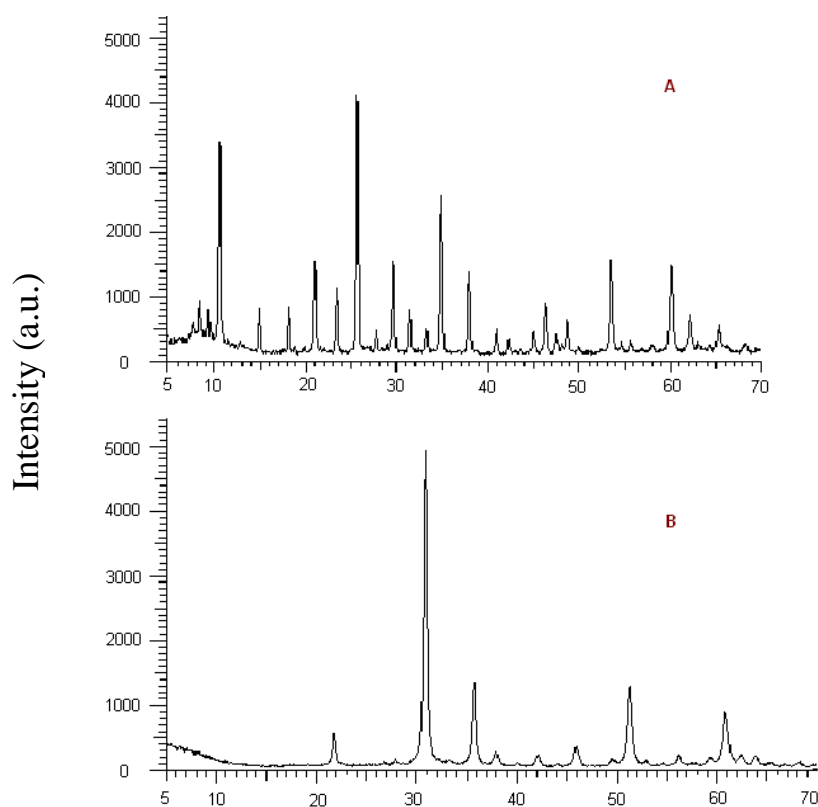


**Figure 5.** The XRD patterns of (a)  $\text{H}_3\text{PW}_{12}\text{O}_{40}$  ;( b)  $\text{H}_3\text{PW}_{12}\text{O}_{40}/\text{In}_2\text{O}_3$  nanocomposite

Diffuse reflectance (DR) UV-Vis spectra showed that the  $\text{H}_3\text{PW}_{12}\text{O}_{40}/\text{In}_2\text{O}_3$  crystallites displayed broad and strong absorption in range of 200-400 nm, which was unlike from the unique  $\text{H}_3\text{PW}_{12}\text{O}_{40}$  and  $\text{In}_2\text{O}_3$  (Fig. 7). The results showed the introduction of the primary Keggin structure into the nanostructure framework.

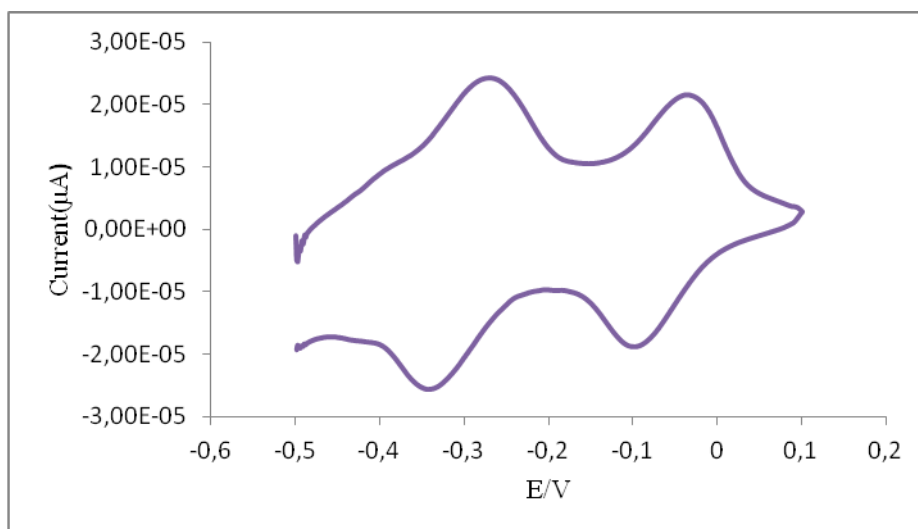


**Figure 6.** Cyclic voltammogram of HPA-  $\text{In}_2\text{O}_3$ -CPE in 0.2 M  $\text{H}_2\text{SO}_4$  solution, Scan rate:  $100 \text{ mV s}^{-1}$ .

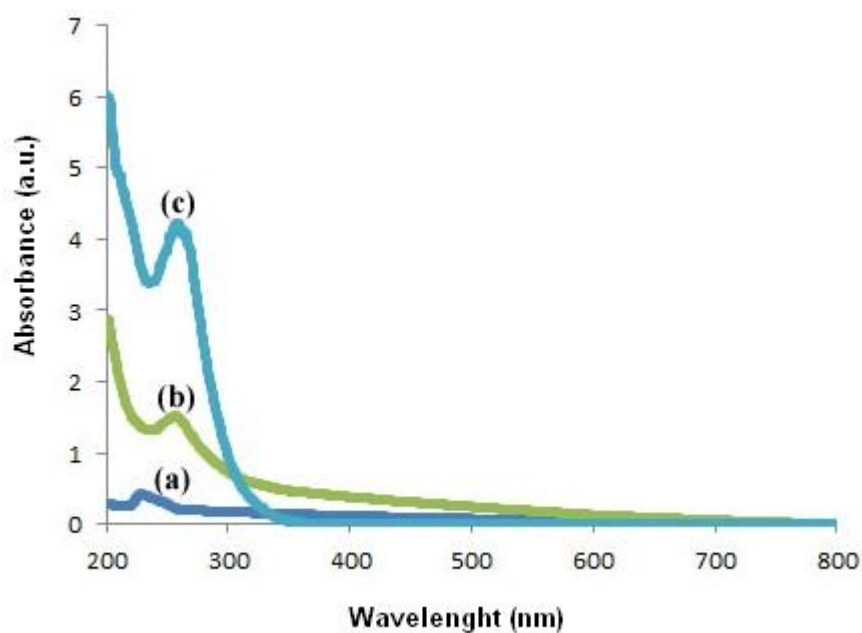


**Figure 7.** DR UV-Vis spectra of: (a)  $\text{In}_2\text{O}_3$  (b)  $\text{H}_3\text{PW}_{12}\text{O}_{40}$ ; and (c)  $\text{H}_3\text{PW}_{12}\text{O}_{40}/\text{In}_2\text{O}_3$

### 3.2. Photocatalytic degradation of dyes

The degradation of Methylene Blue (MB) was studied in aqueous solution under UV-visible light irradiation. Because of the importance of dyes preadsorption before irradiation in photocatalysis experiments, the preadsorption degree of MB by  $\text{H}_3\text{PW}_{12}\text{O}_{40}/\text{In}_2\text{O}_3$  was calculated at ca. 663 nm. The results showed in close proximity to 5% absorption of MB molecules on  $\text{H}_3\text{PW}_{12}\text{O}_{40}/\text{In}_2\text{O}_3$  nanoparticles after 12 h.

**Table 2.** Photocatalytic, sonocatalytic and sonophotocatalytic degradation of dyes catalyzed by HPA-In<sub>2</sub>O<sub>3</sub>.<sup>a</sup>

Dye	In <sub>2</sub> O <sub>3</sub> Photocatalytic			HPA-In <sub>2</sub> O <sub>3</sub> Photocatalytic			HPA-In <sub>2</sub> O <sub>3</sub> Sonocatalytic			HPA-In <sub>2</sub> O <sub>3</sub> Sonophotocatalytic			HPA Photocatalytic			Conc. (ppm)
	Yield (%)	Time (min)	k (min <sup>-1</sup> )	Yield (%)	Time (min)	k (min <sup>-1</sup> )	Yield (%)	Time (min)	k (min <sup>-1</sup> )	Yield (%)	Time (min)	k (min <sup>-1</sup> )	Yield (%)	Time (min)	k (min <sup>-1</sup> )	
Methylene Blue	22±1.6	15	0.105	80±1.2	15	0.12	90±1.4	5	0.46	99±1.3	5	0.92	48±1.4	15	0.044	10
Solophenyl Red-3BL	12.2±1.5	15	0.009	49±1.6	15	0.045	67±1.5	5	0.22	92±1.4	5	0.51	32±1.5	15	0.026	40
Nylosan Black 2-BL-Acid	11.6±1.2	15	0.0082	56±1.4	15	0.055	59±1.3	5	0.18	94±1.6	5	0.56	29±1.7	15	0.023	80
Methyl Orange	8.1±1.3	15	0.0056	26±1.4	15	0.02	30±1.4	5	0.07	78±1.2	5	0.31	20±1.5	15	0.015	20
Bromothymol Blue	10.3±1.3	15	0.0072	44±1.3	15	0.039	50±1.3	5	0.6	85±1.2	5	0.38	23±1.6	15	0.017	40

<sup>a</sup>Reaction conditions: Catalyst (20 mg); Optimum pH; Oxygen flow rate= 5 mL/ min (N=4).

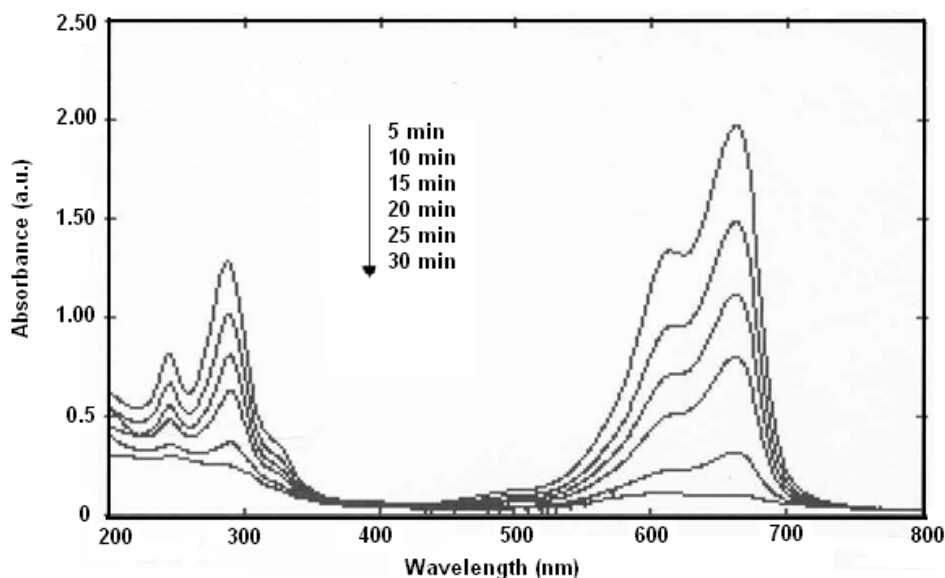


**Figure 8.** Spectral change that occur during photocatalytic degradation of aqueous solution of MB: Catalyst (20 mg); Optimum pH; Oxygen flow rate= 5 mL/ min; Time 5-30 min.

In the photocatalytic experiments, the quantity of catalyst, oxygen flow rate and pH were optimized in the degradation of MB under UV light. The departure of peak at  $\lambda_{max} = 663$  nm was chosen for monitoring of the dye degradation (Fig. 8). The results showed that the degradation percent was 80% in the presence of 20 mg of catalyst and irradiation of UV light for 30 min at room temperature (Table 2). The effect of solution pH was also investigated on the degradation rate of MB. The obtained results showed that the degradation ratio was higher at pH= 4.3 due to the higher degradation ratio and lower stability under neutral and basic aqueous solutions. These optimized situations were used for degradation of different dyes. The effect of pH on the degradation of dyes in

the presence of  $\text{H}_3\text{PW}_{12}\text{O}_{40}/\text{In}_2\text{O}_3$  has been explicated on the basis of point of zero charge ( $\text{pH}_{\text{pzc}}$ ) of  $\text{In}_2\text{O}_3$  particles.  $\text{In}_2\text{O}_3$  has a positive charge in acidic solution and negative charge in alkaline solution. According to this explanation and electrostatic interactions, degradation of the cationic dyes such as MB should be done at alkaline solution, and degradation of anionic dyes such as methyl orange should be completed effectively in acidic solutions.

Results showed that positively and negatively charged dyes are degraded capability in acidic solutions. One possible rationalization for this could be the instability of produced oxidizing agents such as  $\text{H}_2\text{O}_2$  molecules, hence the decrease of dyes degradation in alkaline solutions. However, some suitcases of MB photodegradation in water by UV irradiated  $\text{In}_2\text{O}_3$  at  $\text{pH}=4.3$  has been reported in the literature [20- 23]. According to Shimizu et al, it is complicated to explain the main result of pH [24]. These differences in the optimal pH for the degradation stem from the reliance of the point of zero charge depends on the form of distribution, the difference of diameter and the kind of catalyst. And, as to  $\text{H}_3\text{PW}_{12}\text{O}_{40}/\text{In}_2\text{O}_3$ , the existence of polyoxometalate may change  $\text{pH}_{\text{zpc}}$  which then shows different features from pure  $\text{In}_2\text{O}_3$ . Experiments showed that oxygen is necessary for degradation process. When the reaction takes place without oxygen, only 25% degradation was achieved with a 5 mL/min oxygen gas flow, however, degradation reached its highest level; In other words, this is the existence of oxygen, not the increase in its pressure that can affect the percentage of degradation (%).

In accordance with the Table 2, the  $\text{H}_3\text{PW}_{12}\text{O}_{40}/\text{In}_2\text{O}_3$  is an effective photocatalyst for degradation of organic dye contaminants under irradiation of UV-visible light. However, a plausible pathway for degradation of dyes is displayed in Scheme 1. The difference in the absorption efficiency between  $\text{In}_2\text{O}_3$  and  $\text{H}_3\text{PW}_{12}\text{O}_{40}/\text{In}_2\text{O}_3$  can be exposed by the dyes degradation mechanism catalyzed by  $\text{H}_3\text{PW}_{12}\text{O}_{40}/\text{In}_2\text{O}_3$ . In this mechanism, the reactants (dyes and dioxygen) were brought up to the surface and filled the pores of the composites through diffusion, and then they were adsorbed on the surface and in the pores by a hydrogen bonding interface between efficient groups of dyes and surface hydroxyl groups of  $\text{In}_2\text{O}_3$  support, where they were nearby to the active sites (W– O–W) attached within the pore cavities [25-33].

### 3.3. Sonocatalytic degradation of dyes

Another purpose of the present investigation was the study of the result of ultrasonic irradiation on the dyes degradation by  $\text{H}_3\text{PW}_{12}\text{O}_{40}/\text{In}_2\text{O}_3$ . The increase in irradiation power has no effect on the dye degradation. The existence of  $\text{H}_3\text{PW}_{12}\text{O}_{40}/\text{In}_2\text{O}_3$  ultrasonic system generates  $\text{OH}^\bullet$  in the irradiated solutions. At First, the MB sonodegradation was examined under the reaction situations already illustrated for degradation under UV light (15 mL of 10 ppm MB, 20 mg catalyst,  $\text{pH}=4.3$ , and oxygen flow rate= 5 mL/ min). Irradiation with the ultrasonic waves for 15 min reduced the absorption significantly at 663 nm, which showed a 90% MB degradation under sonication. However, in the presence of  $\text{In}_2\text{O}_3$  under sonication, the MB degradation was achieved only up to 40%. Table 2 displays the capacity of ultrasonic irradiation in the degradation of different dyes. The ultrasound influence is one of the most important parameters that have also a great manipulate on the phenomena of sound cavitation and effectiveness of ultrasound behavior.

Sonocatalytic degradation of dyes in the presence of photocatalysts has been described in several papers. It is mentioned that the oxidation process of dyes is  $\text{OH}^\circ$  in need [33]. Therefore, the presence of  $\text{H}_3\text{PW}_{12}\text{O}_{40}/\text{In}_2\text{O}_3$  in an ultrasonic system should result in the development of  $\text{OH}^\circ$  in the irradiated solutions. Growing in the formation of  $\text{OH}^\circ$  can be explicated by renowned mechanism of hot spots and sonoluminescence.

### 3.4. Sonophotocatalytic degradation of dyes

The application of photocatalysis, sonocatalysis and sonophotocatalysis simultaneously, is more effective than applying their amalgamation successively. Such a permutation produces some extra property and is more effectual than sonolysis and photolysis unaccompanied. It is for this motivation that sonophotocatalytic degradation of dyes was investigated under ultrasonic and UV light irradiation. All reactions were conceded under the same reaction conditions already depicted for photolysis and sonolysis. The results, Table 2, demonstrated that the sonophotocatalytic activity of  $\text{H}_3\text{PW}_{12}\text{O}_{40}/\text{In}_2\text{O}_3$  was higher than those of the straight photolysis and sonolysis by  $\text{In}_2\text{O}_3$ .

### 3.5. Photocatalytic kinetics

As for the investigation of dyes degradation kinetics in aqueous solution under visible ray ultrasonic and amalgamation of visible and ultrasonic beam, MB was used as a substrate model. This model conforms to an apparent first-order in agreement with a generally detected Langmuir-Hinshelwood kinetic model [26]. The determined  $k$  values are summarized in Table 2.

### 3.6. Catalyst Reuse

**Table 3.** The results of HPA-  $\text{In}_2\text{O}_3$  catalyst reuse and W leached in the degradation of MB by photocatalytic, sonocatalytic and sonophotocatalytic.<sup>a</sup>

Run	HPA- $\text{In}_2\text{O}_3$ (Photocatalytic)			HPA- $\text{In}_2\text{O}_3$ (Sonocatalytic)			HPA- $\text{In}_2\text{O}_3$ (Sonophotocatalytic)		
	Yield (%)	Time (min)	W leached <sup>b</sup> (%)	Yield (%)	Time (min)	W leached <sup>b</sup> (%)	Yield (%)	Time (min)	W leached <sup>b</sup> (%)
1	80±1.2	15	1.4	90±1.1	5	1.9	99±1.0	5	1.6
2	78±1.3	15	0.8	89±1.4	5	1.8	98±1.5	5	1.2
3	78±1.6	15	0.4	88±1.5	5	0.8	97±1.4	5	0.9
4	77±1.7	15	0.2	87±1.6	5	0.5	97±1.6	5	0.3

<sup>a</sup>Reaction conditions: Catalyst (20 mg); Optimum pH; Oxygen flow rate= 5 mL/ min.

<sup>b</sup>Determined by ICP(N=4).

At the end of the reaction, the sediment of HPA - $\text{In}_2\text{O}_3$  catalyst was easily recovered by the centrifugation of the suspension, and the improved catalyst was washed with water and ethanol, succeeding. The amount of W leached, in the clear solution, was measured by ICP. The results illustrated that about 2% of W has been leached from catalyst. These results involve strong coordination communications between the Keggin unit and the  $\text{In}_2\text{O}_3$  facade. But, something that is more important is the chemical character of the communication between the Keggin unit and  $\text{In}_2\text{O}_3$  reinforcement. Therefore, the combination could be recycled four times without considerable failure of its photocatalytic activity. The results are abridged in Table 3.

#### 4. CONCLUSIONS

This research introduces a simple and green miscellaneous photocatalytic advance for the degradation of organic dyes which are exploited in the material industry.

The prepared nanocomposite was effectively used for photocatalytic, sonocatalytic and sonophotocatalytic degradation of dissimilar dyes in aqueous media. The elevated catalytic activity of HPA -  $\text{In}_2\text{O}_3$  implies the synergistic consequence between the HPA and the  $\text{In}_2\text{O}_3$ . The HPA -  $\text{In}_2\text{O}_3$  catalyst can be simply separated and recuperated, and deactivation of the catalysts was scarcely viewed after four catalytic recycling.

#### ACKNOWLEDGEMENT

The authors acknowledge the Catalysis Division of Isfahan Payame Noor University (IPNU) and for PNU partial financial support of the present work via the graduate studies fund.

#### References

1. T. Ruther, A.M. Bond, W.R. Jackson, *Green Chem.* 5(2003) 364.
2. Z. Lei, W. You, M. Liu, G. Zhou, S. Takata, M. Hara, K. Domen, C. Li, *Chem Commun.* 9(17) (2003) 2142.
3. S.U.M. Khan, M. Al-Shahry, W.B. Ingler Jr. *Science.* 297 (2002) 2243.
4. A. Fuerte, M.D. Hernandez-Alonso, A.J. Maira, A. Martinez-Arias, M. Fernandez-Garcia, J.C. Conesa, J. Soria, G. Munuera, *J. Catal.* 212 (2002) 1.
5. M. Vautier, C. Guillard, J-M. Herrmann, *J. Catal.* 201 (2001) 46.
6. D. Sattari, C.L. Hill, *J. Chem. Soc. - Chem Commun.* 8 (1990) 634.
7. D. Sattari, C.L. Hill, *J. Am. Chem. Soc.* 115(1993) 4649.
8. H. Einaga, M. Misono, *Bull. Chem. Soc. Jpn.* 69 (1996) 3435.
9. T. Yamase, Takabayashi, M. Kaji, *J. Chem. Soc., Dalton Trans.* (1984) 793.
10. E. Papaconstantinou, *Chem. Soc. Rev.* 18(1989) 1.
11. N.H. Ince, G. Tezcanli, R.K. Belen, I.G. Apikyan, *Appl. Catal. B: Environ.* 29 (2001) 167.
12. M. Saquib, M. Muneer, *Dyes and Pigm.* 56 (2003) 37.
13. M. Muruganandham, M. Swaminathan, *Sol. Energ. Mater. Sol. Cells.* 81 (2004) 439.
14. H. Harada, C. Hosoki, A. Kudo, *J. Photochem. Photobiol. A: Chem.* 141(2001) 219.
15. S. Chaianansutcharit, O. Mekasuwandumrong, P. Prasertam, *Ceram. Int.* 33(2007) 697.

16. C. Rocciccioli-Deltcheff, M. Frank, M. Fournier, R. Thouvenot, *Inorg. Chem.* 22 (1983) 207.
17. A. Chemseddin, C. Sanchez, J. Livage, J. Launay, M. Fournier, *Inorg. Chem.* 23(1984) 2609.
18. S. Tangestaninejad, V. Mirkhani, M. Moghadam, I. Mohammadpoor-Baltork, E. Shams, H. Salavati, *Ultrason. Sonochem.* 15(2008) 438.
19. S. Tangestaninejad, M. Moghadam, V. Mirkhani, I. Mohammadpoor-Baltork, E. Shams, H. Salavati, *Catal. Commun.* 9(2008) 1001.
20. H. Lechheb, E. Puzenat, A. Houas, M. Ksibi, E. Elaloui, C. Guillard, J.M. Herrmann, *Appl. Catal. B: Environ.* 39 (2002) 75.
21. B.N. Lee, W.D. Liaw, J.C. Lou, *Environ. Eng. Sci.* 16(1999) 165.
22. W.S. Kuo, P.H. Ho, *Chemosphere* 45 (2001) 77.
23. T. Zhang, T. Oyama, A. Aoshima, H. Hidaka, J. Zhao, N. Serpone, *J. Photochem. Photobiol. A: Chem.* 140(2001) 163.
24. N. Shimizu, C. Ogino, M.D. Farshbaf, T. Murata, *Ultrason. Sonochem.* 14 (2007) 184.
25. Y. Yang, Q. Wu, Y. Guo, C. Hu, E. Wang, *J. Mol. Catal. A: Chem.* 225 (2005) 203.
26. S. Tangestaninejad, M. Moghadam, V. Mirkhani, I. Mohammadpoor, H. Salavati, *Ultrason. Sonochem.* 15(2008) 815.
27. S. Tangestaninejad, M. Moghadam, V. Mirkhani, I. Mohammadpoor, H. Salavati, *J. Iran. Chem. Soc.* 7(2010) S161.
28. Y. Yang, Q. Wu, Y. Guo, C. Hu, E. Wang, *J. Mol. Catal. A* 225 (2005) 203.
29. D. Carriazo, M. Addamo, G. Marci, C. Martín, L. Palmisano, V. Rives, *Appl. Catal A: Gen* 356 (2009) 172.
30. H. Harada, C. Hosoki, A. Kudo, *J. Photochem. Photobiol. A: Chem* 141(2001) 219.
31. X. Qu, Y. Guo, C. Hu, *J. Mol. Catal A: Chem* 262 (2007) 128.
32. B.R. Jermy, A. Pandurangan, *Appl. Catal A: Gen* 295 (2005) 185.
33. N. Shimizu, C. Ogino, M.D. Farshbaf, T. Murata, *Ultrason. Sonochem.* 14 (2007) 184.